Proceedings of the 11th Brazilian Congress of Thermal Sciences and Engineering -- ENCIT 2006
Braz. Soc. of Mechanical Sciences and Engineering -- ABCM, Curitiba, Brazil,- Dec. 5-8, 2006

Paper CIT06-0412

EXPERIMENTAL PREDICTION OF DEPARTURE FROM NUCLEATE BOILING ON THE IPR-R1 TRIGA NUCLEAR REACTOR CORE

Hugo César Rezende
Centro de Desenvolvimento da Tecnologia Nuclear – CDTN/CNEN
Campus da UFMG – Pampulha. CEP: 30.123-970 - Belo Horizonte/MG
hcr@cdtn.br

Amir Zacarias Mesquita
Centro de Desenvolvimento da Tecnologia Nuclear – CDTN/CNEN
Campus da UFMG – Pampulha. CEP: 30.123-970 - Belo Horizonte/MG
amir@cdtn.br

Abstract. *Experimental and analytical studies have been performed in the IPR-R1 TRIGA Mark-1 Reactor at Technology Development Center (CDTN), Brazil, to find out the temperature distribution as a function of reactor power under steady-state conditions. Initially some studies were made on flow distribution in the coolant channels and heat transfer coefficient on the heated surface (Mesquita, 2005). These results were used for the prediction of departure from nucleate boiling, which defines the limit of fuel heat removal. This paper describes the methodology used and presents the experimental results. The data show the efficiency of the natural circulation to remove the heat generated in by the fissions the IPR-R1 TRIGA core.*

Keywords*. TRIGA Nuclear Reactor, boiling, heat transfer, critical heat flux (CHF).*

1. Introduction

The 250 kW IPR-R1 TRIGA Research Reactor core has a cylindrical configuration with an annular graphite reflector, arranged in a concentric hexagonal array. Figure (1) presents the top view of the reactor core. There are 91 locations in the light-water moderated core, which can be filled either by fuel elements or other components like control rods, a neutron source, irradiation channels, etc. The reactor core has 59 aluminum-clad fuel elements and 5 stainless steel-clad fuel elements, 16 graphite elements, 3 control rods, 2 irradiation channels and a neutron source. Both the kinds of fuel elements use 8.5 wt % uranium at 20 % enrichment. The core configuration and the two hottest coolant channels are presented in Fig. (2). The 5 stainless steel-clad fuel elements contain a pure zirconium rod of 0.635 cm diameter at their center. One of these steel-clad fuel elements, shown in Fig. (3), is instrumented with three thermocouples positioned along its center (Gulf General Atomic, 1972). A graphite reflector enclosed in an aluminum casing surrounds the reactor core. The TRIGA fuel is characterized by inherent safety and high fission product retention.

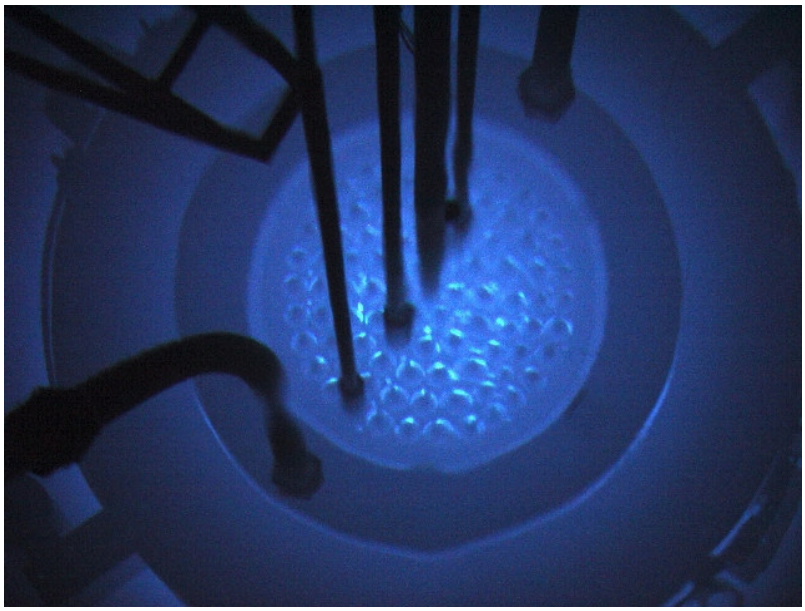

Figure 1. Top View of the TRIGA IPR-R1 core

The forced cooling system of the TRIGA reactor pool is shown in Fig. (4). Like other TRIGA type reactors, the core is cooled by natural circulation. A passage for the cooling water through the top plate is provided by the differential area between a spacer block on the fuel element top and the round hole in the grid. The design accommodates sufficient natural convective flow to maintain continuous bulk subcooled water throughout the core, which thereby avoids significant vapor formation and restricts possible steam bubbles to the vicinity of the fuel element surface. The spacing between adjoining fuel elements, and hence the water fraction in the core, was selected not only from neutronic considerations but also from the thermohydrodynamic considerations.

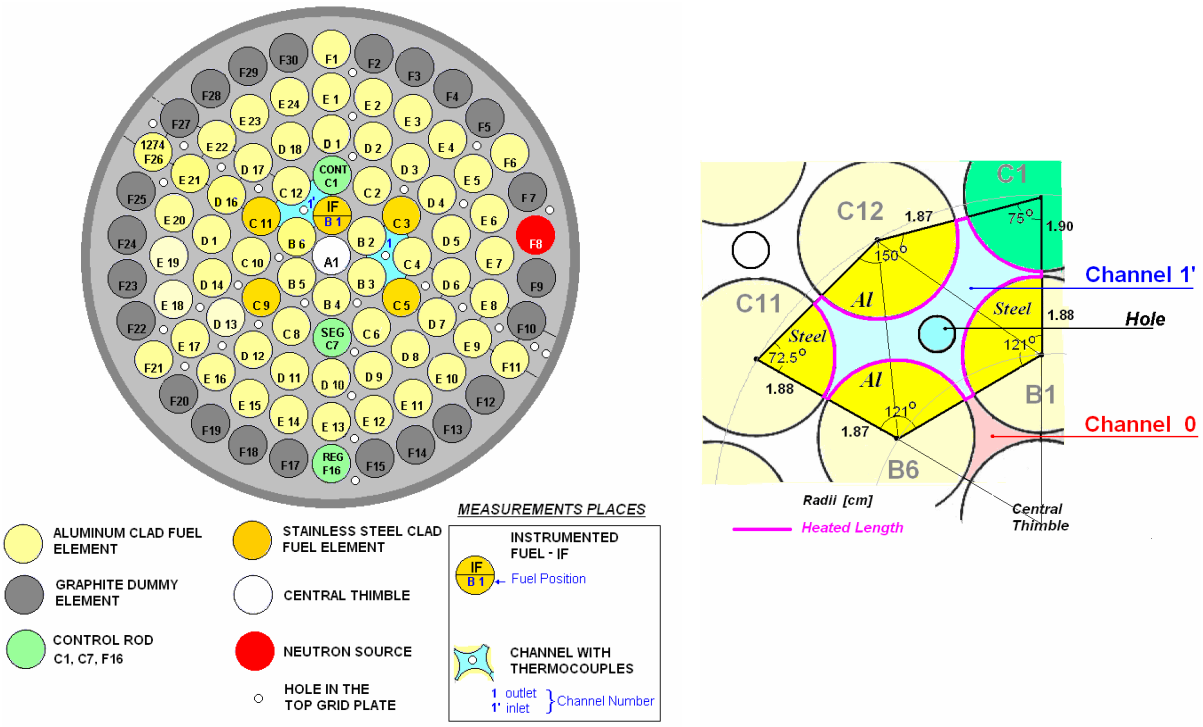

Figure 2. The IPR-R1 core configuration and the two hottest coolant channels

The heat generation by fission in the fuel material is conducted to the coolant through the fuel, through the fuel-cladding interface and through the cladding. The TRIGA reactor power output is limited by three dependent thermal and hydrodynamic variables: the maximum fuel temperature, the departure from nucleate boiling ratio (DNBR) and the core pressure drop. The thermal and hydrodynamic objective of the design is to safely remove the heat generated in the fuel without producing excessive fuel temperatures or steam void formations and without closely approaching the hydrodynamic critical heat flux (CHF) under either steady-state or transient operating conditions. The CHF is the conditions at which the heat transfer coefficient to the two-phase flow coolant deteriorates substantially. For the given flow conditions, it occurs at a sufficiently high heat flux or wall temperature.

The variations in the heat transfer coefficient can be determined by investigating the fuel temperature and the coolant mass flow rate as a function of reactor power. This should provide an accurate prediction about when and where boiling does occur. Certain critical temperatures must not be exceeded within a fuel element to prevent unwanted phase changes. Melting of fuel or cladding must not occur in reactor designs. The heat flux at the cladding surface must not exceed a critical value in order to prevent departure from nucleate boiling. Predictions about when boiling will occur can be made by examining the heat transfer coefficient. The regions of the reactor core where boiling occurs can be determined from the heat transfer coefficient data, at various power levels.

When the heat flux become sufficiently large, the small bubble formed in nucleate boiling coalesce into a vapour film that covers the surface. Since then the heat-transfer efficiency drops dramatically and makes the clad surface temperature to rise by several hundred degrees. The departure from nucleate boiling ratio (DNBR) is used to indicate how close the heat flux is to this critical value. It is defined as the ratio of the critical flux to the actual heat flux in the core. For example, a DNBR of 1.3 implies a safety margin of 30%.

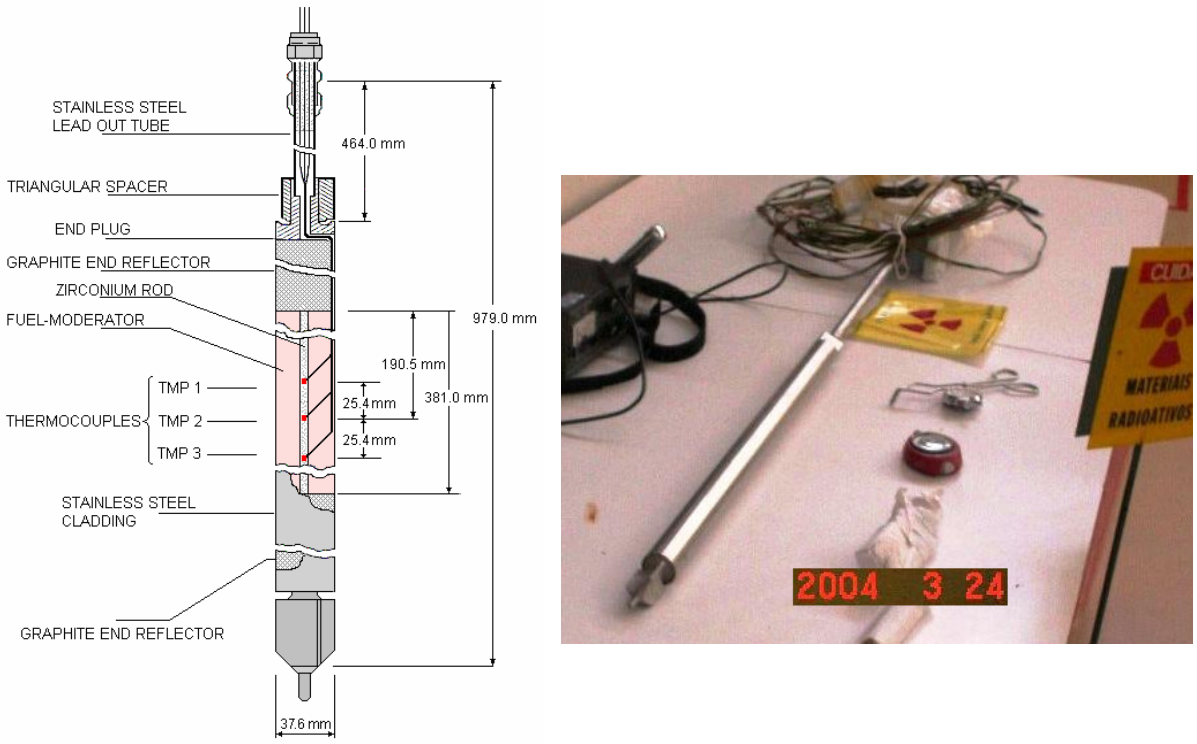

Figure 3. Instrumented fuel element

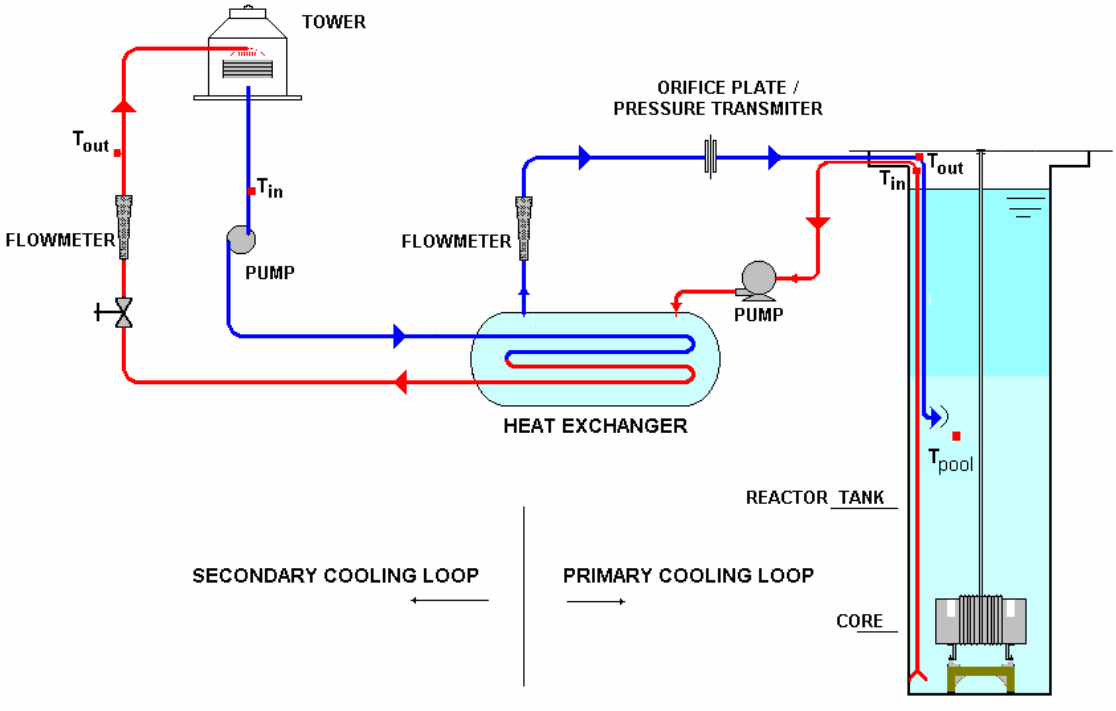

Figure 4. Instrumented fuel element and the reactor cooling system

1. Methodology

Experimental studies have been performed in the IPR-R1 TRIGA Reactor to find out the temperature distribution under steady-state conditions, as a function of reactor power (Mesquita, 2005). The fuel temperature was measured with an instrumented fuel element (Fig. 3), which contains three chromel-alumel (type K) thermocouples. The thermocouples are embedded in the zirconium centerline pin with one thermocouple located at the midplane of the element and the other two 25.5 mm above and below the midplane. Temperature measurements were taken with the instrumented element at location B1 (Fig. 2). This is the hottest fuel element position, predict by the neutronic calculation (Dalle, 1999). Two thermocouples were inserted into the core through some holes in the top grid plate. These thermocouples were placed near position B1 and measure the inlet and outlet temperatures in the channel.

Data are obtained from the console and from a data acquisition system computer that was developed and tested as part of this research project (Mesquita *et al*, 2004). Some of the data collected are power, fuel temperatures, forced water flow and control rod insertion position.

2. Heat transfer regimes from cladding to coolant

Figure (5) presents the typical pool boiling curve on a log-log plot of heat flux versus wall superheat ($T_{sur} - T_{sat}$). At low values of ΔT_{sat} the curve is fairly linear, hence h is relatively constant. There is no bubble formation. Heat transfer is by liquid natural convection. At about ten to twenty degrees above saturation the heat flux increases rapidly with increasing wall temperature. The increase in heat transfer is due to nucleate boiling. The formation of vapor bubbles increases the turbulence near the heated surface and allows mixing of the coolant fluid in the film region, thus enhancing the heat transfer rate. It can be seen from the shape of the curve, that the heat transfer coefficient increases dramatically in the boiling regime. Whenever a solid surface temperature exceeds the saturation, local boiling may occur even if the bulk water temperature is below the saturation temperature. The boundary layer of water on the heated surface can become sufficiently heated so that subcooled pool boiling takes place. The bubbles will condense upon leaving the film region because the bulk water temperature is below the saturation.

By increasing the surface temperature, the heat flux reaches the critical value, where film boiling occurs. In this point the bubbles become so numerous that they form an insulating layer of steam around the fuel element and the heat flux is significantly reduced.

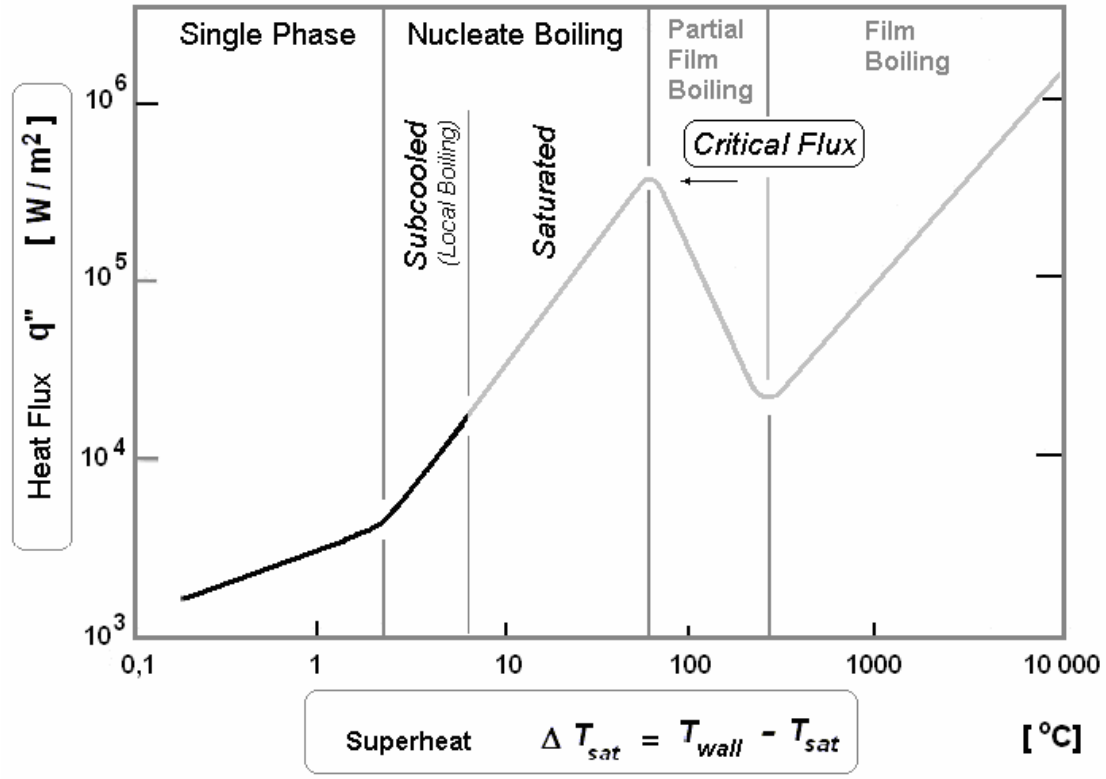

Figure 5. Typical pool boiling curve for water under atmospheric pressure

2.1. Heat transfer coefficient in turbulent single phase flow

Dittus-Boelter (Glasstone and Sesonske, 1994) and (Collier and Thome, 1994) proposed the following correlation to predict heat transfer coefficient (h_{sp}) for turbulent single phase flow in long straight channels in the fully developed region:

$$h_{sp} = \frac{0.023k\, Re^{0.8}\, Pr^{0.4}}{D_w}, \quad \text{or} \quad h_{sp} = 0.023\frac{k}{D_w}\left(\frac{GD_w}{\mu}\right)^{0.8}\left(\frac{c_p\mu}{k}\right)^{0.4} \tag{1}$$

Where: *Re* is the *Reynolds number* and *Pr* the *Prandtl number*, $D_w = 4A/P_w$ is the hydraulic diameter of the channel based on the wet perimeter, A is the flow area in [m^2]; P_w is the wet perimeter in [m]. G is the mass flow in [kg/m^{2}s], c_p is the isobaric specific heat in [J/kgK], k is the thermal conductivity in [W/mK] and μ is the fluid dynamic viscosity in [kg/ms]. The TRIGA IPR-R1 fluid properties are calculated at the bulk water temperature on the sub-saturated region at 1.5 bar.

2.2. Heat transfer coefficient in subcooled nucleate boiling

For local boiling the Newton Equation of cooling is modified to the form:

$$h_b = \frac{q''}{T_{sur} - T_f}, \tag{3}$$

where: h_b is the coefficient for nucleate boiling heat transfer; q'' is the heat transfer rate per unit of surface area [W/m^2]; T_f is the bulk fluid temperature [^{o}C]; T_{sur} is the surface temperature, [^{o}C], given by:

$$T_{sur} = T_{sat} + \Delta T_{sat} \quad . \tag{4}$$

The surface superheat was calculated by the McAdams correlation (Tong and Weisman, 1996), (Huda and Rahman, 2004), (Collier and Thome, 1994):

$$\Delta T_{sat} = 0.81(q'')^{0.259}, \tag{5}$$

with q'' in [W/m^2] e ΔT_{sat} in [^{o}C]. This correlation reproduces experimental data for subcooled water from the temperature of 11 to 83 ^{o}C, from the pressure of 2 to 6 bar; from the velocity of 0.3 to 11 m/s and from the hydraulic diameter of 0.43 cm to 1.22 cm.

3. Critical heat flux and DNBR

In the fully developed nucleate boiling regime it is possible to increase the heat flux without appreciable change in the surface temperature until the point when the bubble motion on the surface becomes so violent that a hydrodynamic crisis occurs. This is the critical heat flux (CHF) with the point of the formation of a continuous vapor film on the surface. In subcooled boiling CHF is a function of the coolant velocity, the degree of subcooling and the pressure. There are a lot of correlations to predict the CHF, the equation used is given by Bernath (Lamarsh and Baratta, 2001). This correlation predicts CHF in the subcooled boiling region and it is based on the critical wall superheat condition at burnout and turbulent mixing convective heat transfer. Bernath's equation gives the minimum results (Obenchain, 1969) so it is the most conservative. It is given by:

$$q''_{crit} = h_{crit}(T_{crit} - T_f) \quad , \tag{6}$$

where,

$$h_{crit} = 61.84\frac{D_w}{D_w + D_i} + 0.01863\frac{23.53}{D_w^{0.6}}u \quad , \tag{7}$$

and,

$$T_{crit} = 57\ln(p-54)\frac{p}{p+0.1034} + 283.7 - \frac{u}{1.219} \quad , \qquad (8)$$

q''_{crit} is the critical heat flux [W/m^2], h_{crit} is the critical coefficient of heat transfer [W/m^{2}K], T_{crit} is the critical surface temperature [^{o}C], T_f is the bulk fluid temperature [^{o}C], p is the pressure [MPa], u is the fluid velocity [m/s], D_w is the wet hydraulic diameter [m], D_i is the diameter of heat source [m]. This correlation is for circular, rectangular and annular channels, pressure of 0.1 to 20.6 MPa, velocity between 1 to 16 m/s and hydraulic diameter of 0.36 to 1.7 cm.

4. Experimental results

As the IPR-R1 TRIGA reactor core power increases, the heat transfer regime from the fuel cladding to the coolant changes from single phase natural convection regime to subcooled nucleate boiling. The hottest measured temperature in the core channel was of 65 ^{o}C (Channel 1'), far below from 111.4 ^{o}C that is the water saturation temperature at 1.5 bar. Therefore the saturated nucleate boiling regime is not reached.

4.1 Heat transfer coefficient

4.1.1. Single-phase

The Dittus-Boelter correlation was used for single phase flow heat transfer (Eq. 1). The analysis was carried out for the two most representative channels. Channel 0 is the hottest channel, located close to the core center, where there is the largest density of neutron flux. It also is the channel around the hottest element in the core (position B1 in Fig. 2), but there is no hole in the top plate in the direction of this channel; so it was not possible to measure its temperature. The temperature in Channel 1' was monitored and the heat transfer coefficients in both channels were estimated using the Dittus-Boelter correlation. The inlet and outlet temperatures in Channel 0 were considered as being the same of Channel 1'. The geometric data of Channel 0 and Channel 1' are given in the Table (1). This table also gives the percentage of power contribution for each fuel for the water temperature increasing along the two hottest channels.

Table 1. Channel 0 and Channel 1' data (Mesquita, 2005)

	Channel 0	**Channel 1'**	**Unit**
Area (A)	1.574	8.214	cm^2
Wet perimeter (P_w)	5.901	17.643	cm
Heated Perimeter (P_h)	3.906	15.156	cm
Hydraulic diameter (D_w)	1.067	1.862	cm
B1 and C1 Fuel Diameter (inox)	3.76	3.76	cm
B6 and C12 Fuel Diameter (Al)	3.73	3.73	cm
C1 Control Rod Diameter	3.80	3.80	cm
Central Thimble	3.81	3,81	cm
Core Total Power (265 kW)	100	100	%
B1 Fuel Contribution	0.54	1.11	%
B6 Fuel Contribution	0.46	0.94	%
C11 Fuel Contribution	-	0.57	%
C12 Fuel Contribution	-	1.08	%
Total Power of the Channel	1.00	3.70	%

Direct measurement of the flow rate in a coolant channel is very difficult because of the bulky size and low accuracy of flow meters. Moreover, it can occur disturbance of velocity profiles, making unwise the extrapolation of the results to other coolant channels. Instead, the flow rate through the core may be determined indirectly from the heat balance across the core using measurements of the water inlet and outlet temperatures. The mass flow rate in the channel is given by the mass flux divided by the channel area. The mass flux is given by thermal balance in the channel:

$$q = \dot{m} c_p \Delta T \,, \tag{6}$$

where: q is the power supplied to the channel in [kW], $\dot{m}$ is the mass flow rate in the channel in [kg/s], c_p is the isobaric specific heat of the water in [J/kgK] and ΔT is the temperature difference between the channel inlet and the outlet in [^{o}C].

Table (2) shows the coolant properties as function of power for the Channels 1' and 0. In the table, G is the mass flux given by $G = \dot{m}$ /*channel area;* u is the velocity given by $u=G/\rho$, where ρ is the water density (995 kg/m^3). The water thermodynamic properties to the IPR-R1 TRIGA are calculated at the bulk water temperature on the sub-saturated at 1.5 bars (Wagner and Kruse, 1998). Table (2) shows in the last column the heat transfer coefficient in single phase flow (h_{sur}), calculated by the Dittus-Boelter correlation.

Table 2. Coolant properties and the single-phase heat transfer coefficient

q Core [kW]	q Channel [kW]	ΔT [^{o}C]	c_p [kJ/kgK]	$\dot{m}$ [kg/s]	G [kg/m^{2}s]	u [m/s]	μ [10^{-3}kg/ms]	k [W/mK]	Re	Pr	h_{sur} [kW/m^2/K]
Canal 1'											
265	9,81	13.9	4.1809	0.169	205.40	0.21	0.549	0.639	6968	3.6	**1.562**
212	7.84	9.6	4.1800	0.195	237.98	0.24	0.575	0.638	7708	3.8	**1.724**
160	5.92	7.0	4.1795	0.202	246.35	0.25	0.596	0.636	7697	3.9	**1.743**
108	4.00	4.6	4.1793	0.208	253.05	0.25	0.620	0.634	7601	4.1	**1.750**
53	1.96	2.5	4.1789	0.188	228.52	0.23	0.638	0.632	6670	4.2	**1.591**
35	1.30	1.8	4.1780	0.172	209.64	0.21	0.642	0.630	6081	4.3	**1.479**
Canal 0											
265	2.65	13.9	4.1809	0.046	289.71	0.29	0.549	0.639	5630	3.6	**2.300**
212	2.12	9.6	4.1800	0.053	335.65	0.34	0.575	0.638	6228	3.8	**2.537**
160	1.6	7.0	4.1795	0.055	347.45	0.35	0.596	0.636	6220	3.9	**2.566**
108	1.08	4.6	4.1793	0.056	356.91	0.36	0.620	0.634	6142	4.1	**2.576**
53	0.53	2.5	4.1789	0.051	322.31	0.32	0.638	0.632	5390	4.2	**2.342**
35	0.35	1.8	4.1780	0.047	295.68	0.30	0.642	0.630	4914	4.3	**2.176**

4.1.2. Subcooled boiling

The heat flux for fully developed subcooled nucleate boiling is given by the equation (Kreith, 2002), (Tong and Tang, 1997):

$$h_{sur} = q'' / \Delta T_{sat} \quad , \tag{4.7}$$

where: h_{sur} is the heat transfer coefficient for local pool boiling between the cladding surface and the coolant [kW/m^{2}K], q'' is the heat flux in fuel surface [kW/m^2] and ΔT_{sat} is the wall superheat [^{o}C]. The h_{sur} as function of the power, with the instrumented fuel element positioned in the Position B1 are shown in the last column of the Table (3).

Table 3. Thermal parameters of the fuel element in the position B1

q_{core} [kW]	q_{B1} [W]	T_o [^{o}C]	q' [W/m]	q'' [W/m^2]	q''' MW/m^3	ΔT_{sat} [^{o}C]	T_{sur} [^{o}C]	k_g **[W/mK]**	h_{sur} **[kW/m^{2}K]**
265	8759	300.6	22988	194613	20.70	19.0	130.4	**10.75**	**10.25**
212	7007	278	18391	155690	16.56	17.9	129.3	**9.84**	**8.69**
160	5288	251.6	13880	117502	12.50	16.7	128.0	**8.94**	**7.05**
108	3570	216.1	9369	79314	8.44	15.0	126.4	**8.31**	**5.27**

4.2. Critical heat flux and DNBR

The closest channel of the reactor center where it is possible to measure the water inlet and outlet temperatures is Channel 1'. The hottest channel is Channel 0, the closest to the center. With the measured temperature values in Channel 1' the value of critical flow was evaluated in these two channels.

The Bernath correlation was used (Eq. 6) for the calculation of the critical heat flux. At the reactor power of 265 kW operating in steady state, the core inlet temperature was 47 ^{o}C. The critical flow for the Channel 0 is about 1,6 MW/m2, giving a DNBR of 8.5. Figure (6) and Figure (7) show the values of DNBR and critical flow for the two channels. The theoretical values found for the TRIGA reactor of the University of New York (General Atomic, 1970) and calculated with the PANTERA code (Veloso, 2005) for the IPR-R1 are also shown. Both theoretical calculations gave smaller results than this experiment. The differences are due to the adopted temperature values. The value of DNBR for Channel 0 possibly is smaller than the found value, therefore the temperatures considered here were collected in Channel 1, that probably have lower temperatures.

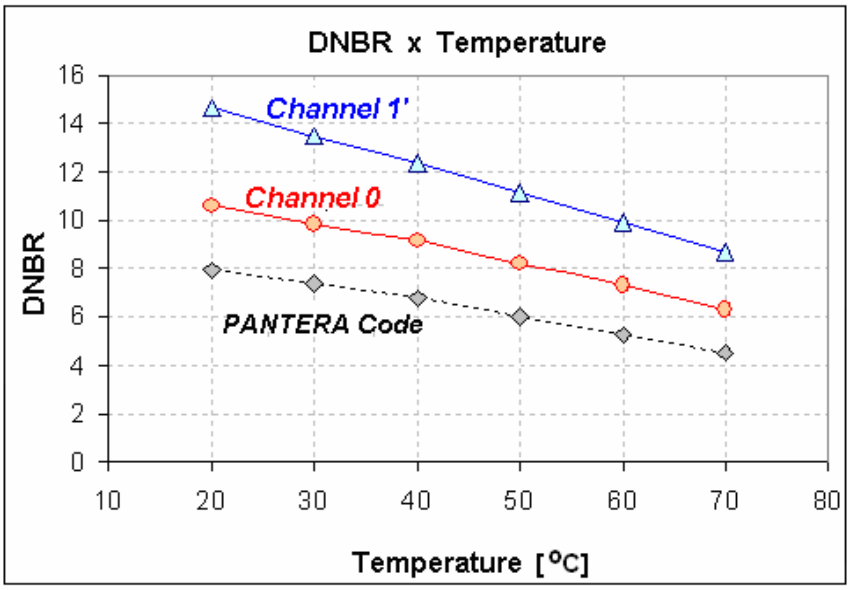

Figure 6. DNBR as a function of the inlet coolant temperature

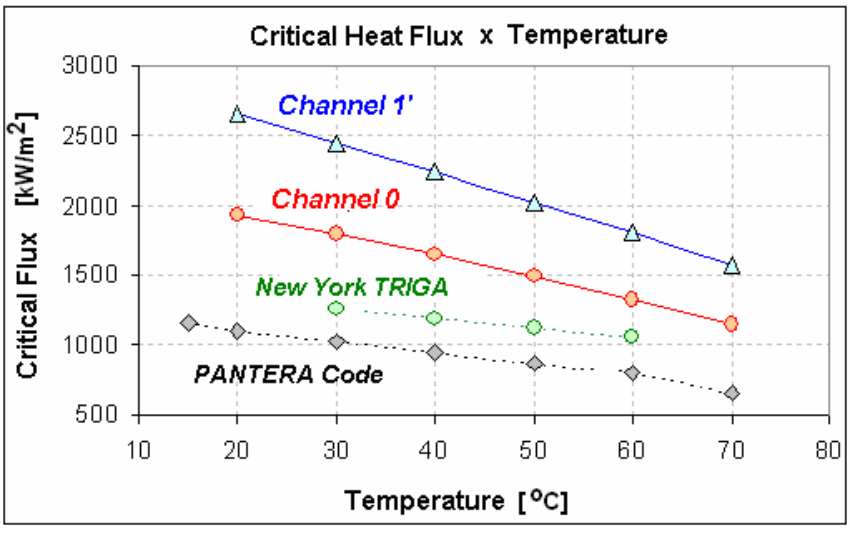

Figure 7. Critical heat flux as a function of the inlet coolant temperature

5. Conclusion

Steady-state studies were performed with the IPR-R1 TRIGA Mark-1 Reactor, to find out the temperature distribution and heat transfer conditions in its core as a function of the reactor power. The resulting minimum DNBR was much larger than other TRIGA reactors. The 2 MW McClellen TRIGA (Jensen and Newell, 1998) has a DNBR=2.5 and the 3 MW Bangladesh TRIGA has a DNBR=2.8 (Huda and Rahman, 2004). Power reactors are projected for a minimum DNBR of 1.3. In routine operation they operated with DNBR close to 2.

The IPR-R1 reactor operates with a great margin of safety in the present power of 250 kW. The maximum heat flux in the hottest fuel is about 8 times lesser than the critical heat flux that would take the hydrodynamic crisis in the fuel cladding. This investigation indicates that the reactor would have an appropriate heat transfer if the reactor operate at the power of 1 MW. The results show the efficiency of the natural circulation to remove the heat generated in the core by the fissions.

However, the high heat transfer coefficient due to subcooled boiling causes the cladding temperature to be quite uniform along most of the fuel rod active region and do not increase very much with the reactor power (Mesquita and Rezende, 2006).

3. Acknowledgement

The authors would like to express their special thanks to the IPR-R1 TRIGA operator team for their help during the experiments.

5. References

Collier, J.G.; Thome, J.R., 1994, "Convective Boiling and Condensation". 3rd. Ed. Clarendon Press, Oxford. 596p.

Dalle, H.M., 1999, "Neutronic calculations of the IPR-R1 TRIGA Reactor with WIMSD4 e CITATION". Belo Horizonte:. Dissertation (M. Sc.). Escola de Engenharia, Universidade Federal de Minas Gerais, (in Portuguese). 183 p.

General Atomic, 1970, "Safeguards Summary Report for the New York University TRIGA Mark I Reactor". (GA-9864). San Diego, 172p.

Glasstone, S. and Sesonske, 1994, "A., Nuclear Reactor Engineering", 4 ed., Chapman and Hall, New York, NY, 805p

Gulf General Atomic, 1972, "15" SST Fuel Element Assembly Instrumented Core". San Diego, CA. Drawing Number TOS210J220.

Huda, M.Q.; Rahman, M., 2004 "Thermo-hydrodynamic Design and Safety Parameter Studies of the TRIGA Mark II Research Reactor". Annals of Nuclear Energy, v. 31, July. p.1102–1118.

Jensen, R.T.; Newell, D.L., 1998, "Thermal hydraulic Calculations to Support Increase in Operating Power in McClellen Nuclear Radiation Center (MNRC) TRIGA Reactor". Proceedings of 1988 RELAP5 International User´S Seminar. College Station, Texas, USA.

Kreith, F. and Bohn, M. S., 2001, "Principles of Heat Transfer", 6th ed., Brooks/Cole, New York, 568p.

Lamarsh, J.R. and Baratta, A.J., 2001, "Introduction to Nuclear Engineering", 3° ed., Upper Saddler River: Prendice Hall, 783p.

Mesquita, A. Z., 2005, "Experimental Investigation on Temperatures Distribuitions in a Research Nuclear Reactor TRIGA IPR-R1", Ph.D thesis, Universidade Estadual de Campinas, São Paulo, (in Portuguese), 174p.

Mesquita, A.Z.; et al, 2004, "Data Acquisition and Signal Processing System for IPR R1 TRIGA Mark I Nuclear Research Reactor of CDTN". Proceedings of 2nd. World Triga Users Conference. Atominstitute Vienna, Austria.

Mesquita, A.Z and Rezende, H.C., 2006, "Experimental Thermal-Hydraulic Analysis of the IPR-R1 TRIGA Nuclear Reactor". Proceedings of the 11th Brazilian Congress of Thermal Sciences and Engineering -- ENCIT 2006, Braz. Soc. of Mechanical Sciences and Engineering - ABCM, Curitiba, Brazil,- Dec. 5-8.

Obenchain, C.F., 1969, "PARET- A Program for the Analysis of Reactor Transients", IDO–17282.

Tong, L. S. and Tang, Y.S, 1997, "Boiling Heat Transfer and Two-Phase Flow", 2nd. Ed. Taylor & Francis, Washington, 542p.

Tong, L.S. and Weisman, J., 1996, "Thermal Analysis of Pressurized Water Reactors", Third Edition, American Nuclear Society. Illinois,748p.

Veloso, M.A., 2005, Thermal–hydraulic Analysis of the IPR-R1 TRIGA Reactor in 250 kW, CDTN/CNEN, NI-EC3-05/05, Belo Horizonte, (in Portuguese), 166p.

Wagner, W. and Kruse, A., 1998, "Properties of Water and Steam – The Industrial Standard IAPWS-IF97 for the Thermodynamics Properties", Springer, Berlin, 354p.

6. Copyright Notice